De Novo Mutations Activating Germline *TP53* in an Inherited Bone-Marrow-Failure Syndrome

Tsutomu Toki,[1,20] Kenichi Yoshida,[2,3,20] RuNan Wang,[1,4,20] Sou Nakamura,[5,20] Takanobu Maekawa,[6] Kumiko Goi,[7] Megumi C. Katoh,[8,9] Seiya Mizuno,[9] Fumihiro Sugiyama,[9] Rika Kanezaki,[1] Tamayo Uechi,[10] Yukari Nakajima,[10] Yusuke Sato,[2,3] Yusuke Okuno,[2,11] Aiko Sato-Otsubo,[2,3] Yusuke Shiozawa,[3] Keisuke Kataoka,[3] Yuichi Shiraishi,[12] Masashi Sanada,[2,3] Kenichi Chiba,[12] Hiroko Tanaka,[13] Kiminori Terui,[1] Tomohiko Sato,[1] Takuya Kamio,[1] Hirotoshi Sakaguchi,[11] Shouichi Ohga,[14] Madoka Kuramitsu,[15] Isao Hamaguchi,[15] Akira Ohara,[16] Hitoshi Kanno,[17] Satoru Miyano,[12,13] Seiji Kojima,[11] Akira Ishiguro,[18] Kanji Sugita,[7] Naoya Kenmochi,[10] Satoru Takahashi,[8,9] Koji Eto,[5] Seishi Ogawa,[2,3,19,21,*] and Etsuro Ito[1,21,*]

Inherited bone-marrow-failure syndromes (IBMFSs) include heterogeneous genetic disorders characterized by bone-marrow failure, congenital anomalies, and an increased risk of malignancy. Many lines of evidence have suggested that p53 activation might be central to the pathogenesis of IBMFSs, including Diamond-Blackfan anemia (DBA) and dyskeratosis congenita (DC). However, the exact role of p53 activation in each clinical feature remains unknown. Here, we report unique *de novo TP53* germline variants found in two individuals with an IBMFS accompanied by hypogammaglobulinemia, growth retardation, and microcephaly mimicking DBA and DC. *TP53* is a tumor-suppressor gene most frequently mutated in human cancers, and occasional germline variants occur in Li-Fraumeni cancer-predisposition syndrome. Most of these mutations affect the core DNA-binding domain, leading to compromised transcriptional activities. In contrast, the variants found in the two individuals studied here caused the same truncation of the protein, resulting in the loss of 32 residues from the C-terminal domain (CTD). Unexpectedly, the p53 mutant had augmented transcriptional activities, an observation not previously described in humans. When we expressed this mutant in zebrafish and human-induced pluripotent stem cells, we observed impaired erythrocyte production. These findings together with close similarities to published knock-in mouse models of *TP53* lacking the CTD demonstrate that the CTD-truncation mutations of *TP53* cause IBMFS, providing important insights into the previously postulated connection between p53 and IBMFSs.

Inherited bone-marrow-failure syndromes (IBMFSs) include a heterogeneous group of genetic disorders characterized by bone-marrow failure, congenital anomalies, and an increased risk of malignacy.[1] Many lines of evidence suggested that p53 activation may be central to the pathogenesis of IBMFSs, including Diamond-Blackfan anemia (DBA [MIM: 105650]) and dyskeratosis congenita (DC [MIM: 305000]).[2,3]

DBA is characterized by macrocytic pure red-cell aplasia involving a decreased number of erythroid progenitors in the bone marrow and various constitutive abnormalities.[4] Except for rare germline *GATA1* (MIN: 305371) mutations,[5] all known causative mutations involve ribosomal protein (RP) genes.[6] It is widely accepted that the pathogenesis of DBA involves elevated p53 accumulation caused by haploinsufficiency of a ribosomal component; this haploinsufficiency leads to an increased stability of the protein by an MDM2-mediated mechanism, thereby inducing cell-cycle arrest and apoptosis of erythroid precursors.[2] DC is caused by germline mutations in the telomerase complex or the shelterin telomere protection complex.[7] An individual with DC typically presents with a classic triad of phenotypes, including nail dystrophy, oral leukopathies, and skin hyperpigmentation. However, these phenotypes are usually not evident until the second decade of life. In most DC cases, the initial hematologic abnormalities

[1]Department of Pediatrics, Hirosaki University Graduate School of Medicine, Hirosaki 036-8562, Japan; [2]Cancer Genomics Project, Graduate School of Medicine, the University of Tokyo, Tokyo 113-00333, Japan; [3]Department of Pathology and Tumor Biology, Graduate School of Medicine, Kyoto University, Kyoto 606-8501, Japan; [4]Department of Pediatrics, Shengjing Hospital of China Medical University, Shenyang 110004, Liaoning, China; [5]Department of Clinical Application, Center for iPS Cell Research and Application, Kyoto University, Kyoto 606-8507, Japan; [6]Department of General Pediatric and Interdisciplinary Medicine, National Center for Child Health and Development, Tokyo 157-8535, Japan; [7]Department of Pediatrics, Faculty of Medicine, University of Yamanashi, Yamanashi 409-3898, Japan; [8]Department of Anatomy and Embryology, Faculty of Medicine, University of Tsukuba, Tsukuba 305-8575, Japan; [9]Laboratory Animal Resource Center, Faculty of Medicine, University of Tsukuba 305-8575, Japan; [10]Frontier Science Research Center, University of Miyazaki, Miyazaki 889-1692, Japan; [11]Department of Pediatrics, Nagoya University Graduate School of Medicine, Nagoya 466-8550, Japan; [12]Laboratory of DNA Information Analysis, Human Genome Center, Institute of Medical Science, the University of Tokyo, Tokyo 108-8639, Japan; [13]Laboratory of Sequence Analysis, Human Genome Center, Institute of Medical Science, the University of Tokyo, Tokyo 108-8639, Japan; [14]Department of Pediatrics, Graduate School of Medical Sciences, Kyushu University, Fukuoka 812-8582, Japan; [15]Department of Safety Research on Blood and Biological Products, National Institute of Infectious Diseases, Tokyo 208-0011, Japan; [16]Department of Pediatrics, Omori Medical Center, Toho University, Tokyo 143-8540, Japan; [17]Department of Transfusion Medicine and Cell Processing, Tokyo Women's Medical University, Tokyo 162-8666, Japan; [18]Division of Hematology, National Center for Child Health and Development, Tokyo 157-8535, Japan; [19]Department of Medicine, Karolinska Institute, Center for Hematology and Regenerative Medicine, SE-171 76 Stockholm, Sweden
[20]These authors contributed equally to this work
[21]These authors contributed equally to this work
*Correspondence: sogawa-tky@umin.ac.jp (S.O.), eturou@hirosaki-u.ac.jp (E.I.)
https://doi.org/10.1016/j.ajhg.2018.07.020.

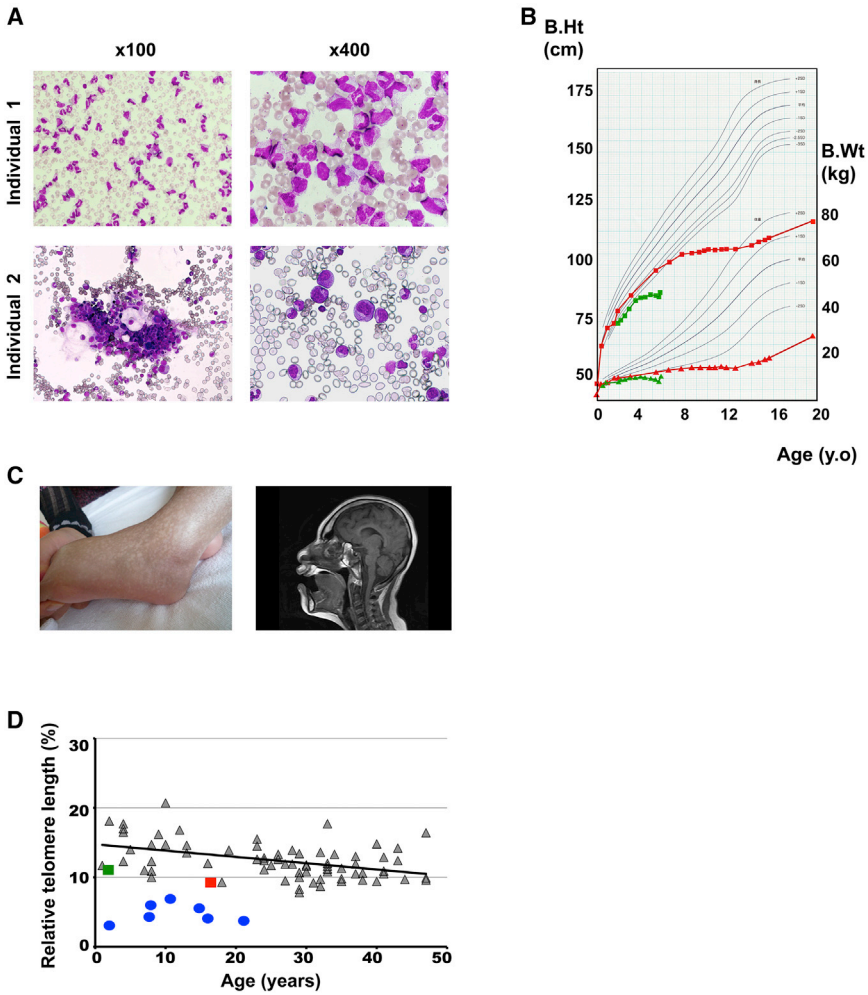

Figure 1. Clinical Features of the Individuals

(A) Bone-marrow smears from individual 1 (top) and individual 2 (bottom) show selective erythroid hypoplasia.

(B) Growth curves of individual 1 (red) and individual 2 (green) exhibit marked growth retardation.

(C) Reticular skin pigmentation and severe microcephaly as demonstrated by magnetic resonance imaging noted in individual 1 at 16 years of age.

(D) Telomere lengths in peripheral blood lymphocytes from individual 1 (red) and individual 2 (green) compared to normal individuals (gray) (median age, 29 years; range, 1–47 years) and an individual with DC (blue); telomere lengths were estimated by flow-cytometry fluorescent *in situ* hybridization (flow-FISH) and expressed as the FISH signals relative to the signal from a normal control (1301 cell line).

include thrombocytopenia or macrocytic anemia followed by pancytopenia.[1] Hypogammaglobulinemia is also common.[8,9] It is widely accepted that telomere or telomerase dysfunction in DC leads to uncapped chromosomes, resulting in p53 activation and induction of apoptosis.[3]

Although the p53 pathway appears to be a critical mediator in both diseases, the exact role of p53 activation in each clinical feature remains unknown. In this report, we describe two individuals with a unique form of IBMFS caused by *de novo* germline mutation of *TP53* (MIM: 191170), unequivocally suggesting a role of augmented p53 functions in the pathogenesis of bone-marrow failure.

The two individuals in our DBA cohort had similar clinical phenotypes that partially mimicked DBA (e.g., pure red-cell aplasia [Figure 1A] and growth retardation [Figure 1B]).[4] Other features, such as hypogammaglobulinemia and microcephaly (Figure 1C), are also seen in DBA[4,10] but are more common in DC.[8] In fact, the older case (individual 1) presented typical DC-like features, including reticular skin pigmentation (Figure 1C), hypogonadism, and tooth anomalies (Table 1) (see Supplemental Note).[9] Their anemia did not respond to steroid therapy. They required a regular blood transfusion from early infancy. However, anemia of individual 1 showed spontaneous remission at 13 years of age, and he became transfusion independent. Both individuals needed regular IgG replacement therapy for persistent hypogammaglobulinemia. No cancers were identified in either individual. No mutations or deletions were detected in the known DBA-associated genes. To identify causative mutations, we first performed whole-exome sequencing (WES) of germline DNA obtained from the peripheral blood of the two individuals and their parents and/or siblings as previously described (Supplemental Material and Methods).[12] Gene mutations were confirmed by Sanger sequencing, performed with their hair follicles and/or buccal tissues. Written informed consent was obtained from their parents. The ethics committees at Hirosaki University and the University of Tokyo approved this study. In WES and copy-number analysis, we did not find mutations or deletions in the genes associated with IBMFSs (Tables S1 and S2). Intriguingly, however, in both individuals we identified heterozygous frameshift variants commonly affecting *TP53* (c.1083delG in individual 1 [II-3] and c.1077delA in individual 2 [II-3]: RefSeq accession: NM_001126112.2) (Figure 2A). These *TP53* mutations were not found in their parents (Figure 2A and 2B), indicating that both variants represented *de novo* germline mutations. These frameshift mutations led to identical C-terminal truncations (p.Ser362Alafs*8) (Figure 1C). Both variants were located in exon 10, resulting in the introduction of premature terminal codons in the last coding exon (exon 11) (Figure 1D). Therefore, mutant transcripts most likely escaped from the nonsense-mediated mRNA decay pathway.[13] Indeed, Sanger sequencing detected the mutant transcripts in amounts comparable to

Table 1. Clinical Characteristics of ΔCTD Mutant Mice and the Individuals Carrying a *TP53*-ΔCTD Allele

	Individuals		Mice (No. Analyzed)		Reported Frequencies in	
	1	2	$p53^{\Delta 31/\Delta 31}$ [22]	$p53^{\Delta 24/\Delta 24}$ [23]	DBA[1,4,11]	DC[1,8,9,11]
Age at diagnosis	2 m	15 d	NA	NA	NA	NA
Gender	M	M	NA	NA	NA	NA
Bone-Marrow Failure						
PRCA	+	+	−	−	~100%	+[d]
Pancytopenia	−	−	+	+	−	>95%
Aplasia in BM	+[a]	+[a]	+ (8/8)	+	+[a]	+
Spontanous remission	+	−	−	−	20%	ND
Physical Anomalies						
Microcephaly	+	+	+	+	reported	6%
Growth retardation	+	+	+ (16/25)	+	30%	20%
Mental retardation	+	+	ND	ND	reported	25%
Hypogonadism	+	ND	+ (10/11)	ND	reported	6%
Physical Anomalies Associated with DC						
Pulmonary fibrosis	−	−	+ (7/8)	ND	ND	20%
Nail dystrophy	−	−	+ (2/8)	ND	ND	88%
Oral leukoplakia	−	−	+ (8/8)	ND	ND	78%
Skin hyperpigmentation	+	−	+ (25/25)	+	ND	89%
Teeth abnormal	+	−	ND	ND	ND	17%
Abnormal Laboratory Findings						
Hypogammaglobulinemia	+	+	ND	ND	rare	common
Telomere shortening	+[b]	+[b]	+	ND	+[b]	100%[c]

Abbreviations are as follows; d: day, m: month, y: year, M; male, NA: not applicable, PRCA: pure red cell aplasia, ND: not described.
[a]Aplasia is limited to erythroid lineage in BM.
[b]Telomere length is between the 1st and 10th percentile.
[c]Most patients with DC have very short telomeres, less than 1st percentile (< 1%).
[d]In most cases with DC, the initial hematologic abnormalities are thrombocytopenia or macrocytic anemia followed by pancytopenia.

those of normal transcripts in peripheral blood mononuclear cells (PBMCs) from individual 1 (Figure S1). A spontaneous remission of the IBMF phenotype within the second decade of life in individual 1 suggests the possibility of a clonal genetic reversion event. However, deep sequencing showed comparable variant allele frequency (VAF) of the *TP53* mutation in PBMC in remission (VAF: 0.49).

TP53 is a tumor-suppressor gene most frequently mutated in human cancers; occasional germline variants also occur in Li-Fraumeni cancer-predisposition syndrome (LFS [MIM: 151623]).[14,15] Most of these mutations affect the core DNA-binding domain, leading to compromised transcriptional activities.[16] In contrast, the variants found in two individuals showed the same protein truncations, resulting in the loss of 32 residues from the C-terminal domains (CTDs) (Figure 2C). Significantly, no mutations involving the CTD have been reported in human cancers or LFS according to the International Agency for Research on Cancer TP53 database v.R18, which compiles >29,000 somatic mutations in cancer and >880 germline mutations.[16] Furthermore, we could not find IBFMS cases with the CTD-truncating mutations of *TP53* in the published literature. To test whether the loss of the CTD affected the transcriptional activities of p53, we first assessed the transcriptional activity of the p53 mutant seen in two individuals by luciferase assay involving the promoter of *CDKN1A* as described in the Supplemental Material and Methods. The transcriptional activation of the mutant was significantly higher than that of wild-type p53 (Figure 2E), suggesting that the variants found in both individuals were activating mutations.

To investigate the biological effects of the *TP53* mutations *in vivo*, we developed zebrafish expressing a CTD-truncated p53. Thus, using one-cell-stage embryos, we injected a Morpholino antisense oligo (MO) that targeted the 3′ splice site of intron 10 (spMO) (Figure 3A and Supplemental Material and Methods). The MO-injected embryos were grown at 28.5°C. Total RNA was isolated from wild-type and MO-injected embryos at 8 hr post-fertilization (hpf). Reverse transcription (RT)-PCR was used for

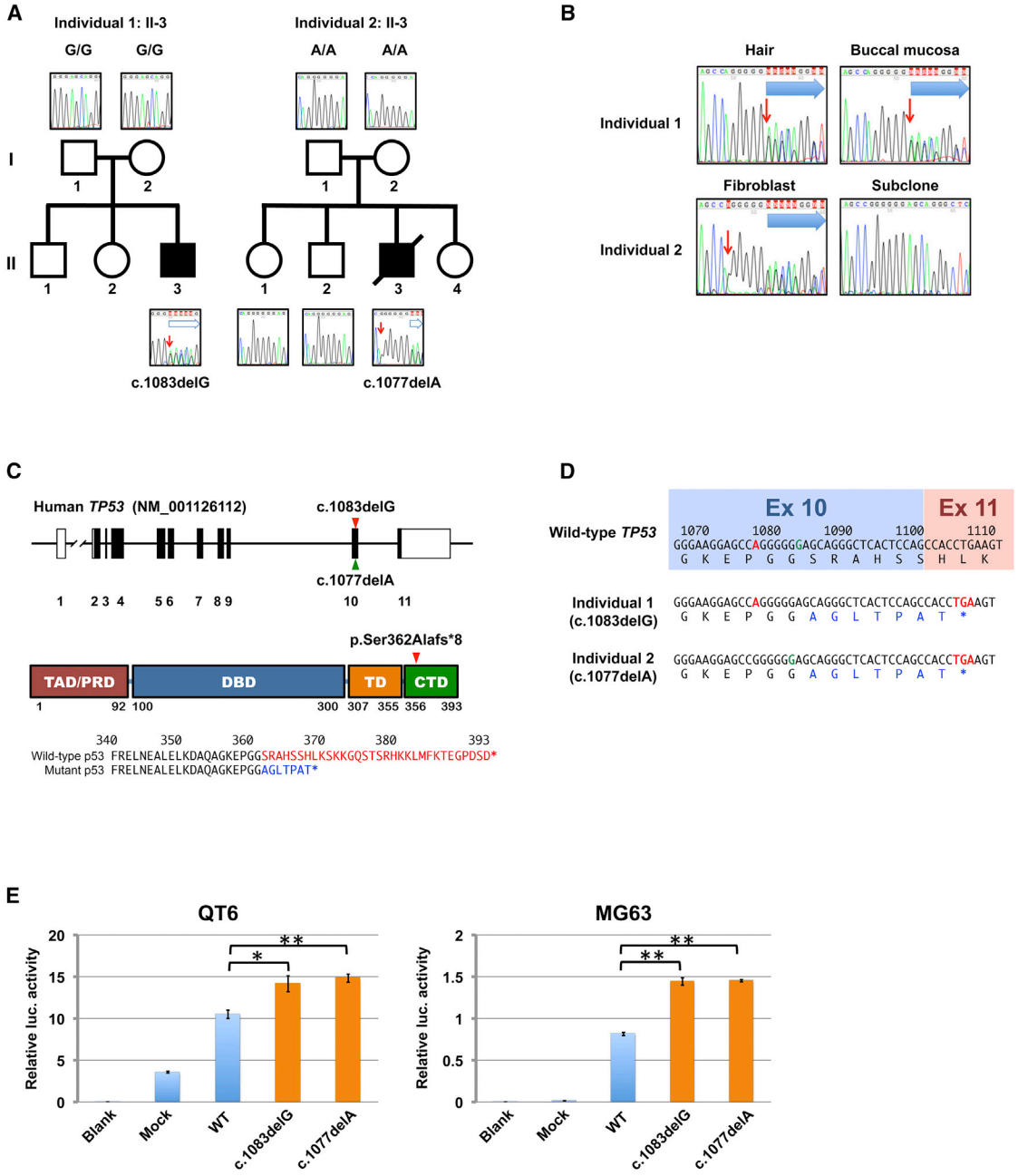

Figure 2. ***TP53*** **Gene Alteration Observed in Individuals with Inherited Bone-Marrow-Failure Syndrome**

(A) Pedigrees for individuals 1 (left) and 2 (right). Each individual had a *de novo* germline mutation. The red arrows indicate the positions of the single-nucleotide deletions. Blue arrows indicate the frameshift signals.

(B) The *TP53* mutation in different tissues from individuals 1 and 2. The right lower panel shows the DNA sequences of the subcloned molecule derived from individual 2, demonstrating the deletion of c.1077A. Red arrows indicate positions of the single-nucleotide deletion. Blue arrows indicate the frameshift signals.

(C) Structure of the *TP53* locus in which the locations of the mutations in individual 1 (red) and individual 2 (green) are indicated by arrowheads (top). Structure of human p53 consisting of domains for transactivation (TAD), specific DNA binding (DBD), and tetramerization (TD), as well as proline-rich (PRD) and C-terminal (CTD) domains (middle). The two heterozygous frameshift variants in *TP53* in individuals 1 and 2 resulted in identical C-terminal truncations (arrowhead). A comparison of the amino acid sequences of the C termini of the wild-type and mutant p53s is shown (bottom). Deleted or altered sequences in p53 variants in both individuals are shown in red and blue, respectively.

(D) The position of *TP53* c.1077A is shown in red and c.1083G in green. c.1083G was deleted in individual 1, c.1077A was deleted in individual 2, and both translated products had identical amino acid sequences. Altered amino acid residues are indicated in blue. Both variants in exon 10 resulted in the introduction of premature terminal codons in the last coding exon (exon 11).

(E) Luciferase activities from a *CDKN1A* promoter co-transduced with indicated constructs in QT6 (left) and MG63 (right) cell lines. Blank: no DNA. MOCK: mock vector. WT: wild-type *TP53*. c.1083delG: c.1083delG *TP53* variant. c.1077delA: c.1077delA *TP53* variant. *$p < 0.01$; **$p < 0.001$, t test. Error bars indicate standard deviation.

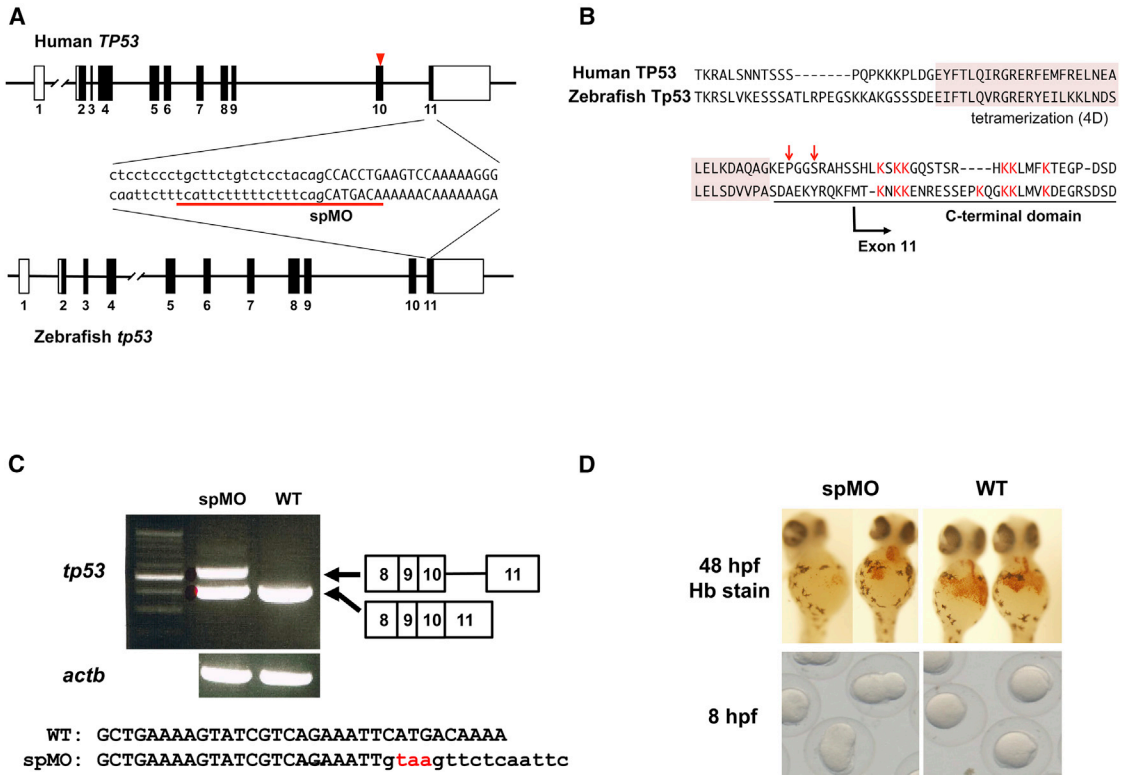

Figure 3. Functional Analyses Based on a Zebrafish Model

(A) The structures of human *TP53* and zebrafish *tp53*. The sequences at the intron 10/exon 11 boundary regions are indicated. Uppercase and lowercase letters show the exon and intron sequences, respectively. The MO target site is underlined. The arrowhead indicates the position of the mutated nucleotides in the affected individuals.

(B) The amino acid sequences of the C-terminal regions of human TP53 and zebrafish Tp53. The conserved lysine residues in the CTD for human and zebrafish are shown in red. The arrows indicate the positions of the mutant nucleotides in the individuals. The tetramerization domain is shaded in pink.

(C) RT-PCR-based detection of *tp53* and *actb* in MO-injected and wild-type embryos. A larger transcript retaining intron 10 is detected in the MO-injected embryos. Injection of spMO perturbed the splicing of intron 10 and introduced a premature stop codon just after exon 10, leading to the elimination of the lysine-rich CTD in Tp53.

(D) Representative hemoglobin staining of cardial veins at 48 hpf and cell divisions at 8 hpf found in MO-injected and wild-type embryos. Approximately 40% of the embryos injected with spMO at 2.5 μg/μL show a severe to moderate reduction of erythrocytes. The injection of MO at 5 μg/μL led to developmental arrest at 8–9 hpf.

distinguishing normal and intron-containing sizes of the *tp53* transcripts. Injection of spMO into the one-cell-stage embryos perturbed the splicing of intron 10 and introduced a premature stop codon just after exon 10, leading to the elimination of the lysine-rich CTD in Tp53 (Figures 3B and 3C). The spMO-injected embryos presented developmental defects with severe morphological abnormalities and died by 96 hpf. Hemoglobin staining at 48 hpf reflected reduced erythrocyte production in the cardial vein of the embryos (Figure 3D). These results suggest that the CTD-truncated p53 perturbed the early development and erythrocyte production of zebrafish.

To further examine the effects of the mutated *TP53* in human cells, we used CRISPR/Cas9-mediated gene editing (Supplemental Material and Methods) to establish a human-induced pluripotent stem cell (hiPSC) line carrying a heterozygous *TP53* mutant allele (Figure 4A). We prepared the plasmids expressing CRISPR guide RNA and Cas9 by ligating oligos into the BbsI site of pX330 (Addgene no. 42230). We designed the candidate sequences for CRISPR guide RNA by using UCSC Genome Browser to introduce frameshift mutations in the CTD of *TP53*. The targeting constructs for genome editing and neomycin resistance gene expression plasmids were transfected into hiPSCs #8[17] and selected with neomycin (G418). We confirmed significantly elevated expression of the downstream targets of p53 in the mutant hiPSCs compared to isogeneic wild-type iPSCs, for all the targets tested, including *CDKN1A* (OMIN: 116899), *MDM2* (OMIN: 164785), *PMAIP1* (OMIM: 604959), and *TIGAR* (OMIN: 610775) (Figure 4B). We then assessed the ability of the mutant hiPSCs to produce erythroid lineage cells upon induced erythroid differentiation as previously reported (Figure 4C).[17] Twelve and 18 days after induction, the number of CD71- and glycophorin-A-positive cells was significantly lower in mutant hiPSCs than in the isogenic control (Figure 4D and Table S3). These results suggest that hiPSCs carrying the heterozygous *TP53* mutations

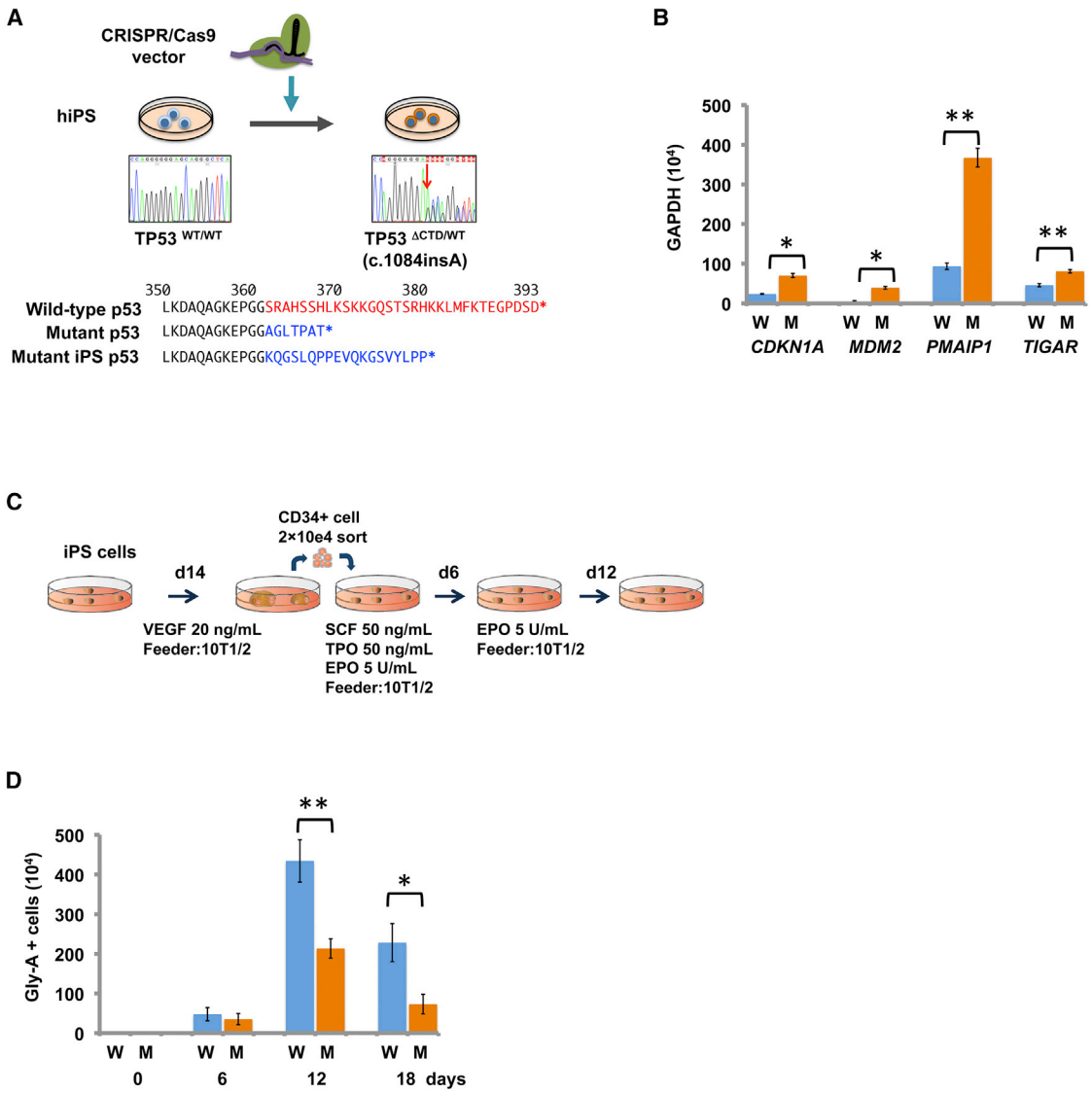

Figure 4. Functional Analyses Based on a Human iPSC Model

(A) An hiPSC line carrying a heterozygous *TP53* mutant allele was generated by CRISPR/Cas9-mediated gene editing (upper). Comparison of the amino acid sequences of the C termini of wild-type and mutant p53s in the affected individuals and mutant hiPSC (bottom). Deleted or altered sequences in p53 variants in both individuals and the mutant hiPSC are shown in red and blue, respectively.

(B) Comparison of the expression of four downstream targets of p53 in the mutant hiPSC (M) and isogenic control (W) by real-time quantitative RT-PCR. Error bars indicate standard deviation.

(C) Scheme for differentiation of erythroid lineage from hiPSCs. To differentiate hiPSCs into erythroid cells, we used our previously established protocol.[16]

(D) Effects of the truncating p53 mutant on erythropoiesis as measured by the numbers of glycophorin-A (Gly-A)-positive cells after *in vitro* erythroid induction. The combined results of three independent experiments are shown. *$p < 0.01$; **$p < 0.001$, t test. Error bars indicate standard deviation.

possess enhanced p53 activity and impaired erythroid differentiation.

In response to a variety of stresses, p53 undergoes extensive post-translational modification, including phosphorylation and acetylation. The CTD is subjected to multiple and diverse post-translational modifications that are thought to be essential for the regulation of p53 stability and activity.[18] Although the precise roles and functions of the p53 CTD are not fully understood,[19] the p53 CTD has been shown to act as a docking site for negative regulators such as Smyd2 and SET.[20,21] Thus, the deletion of the CTD might result in compromised binding of these p53 variants to the negative regulators and impairment of their transcriptional repression.

Recent studies using mouse models demonstrated that the CTD plays key roles in postnatal homeostasis of the hematopoietic compartment and development of the brain.[22,23] Simeonova et al. described a genetically engineered mouse carrying a mutant *Tp53* knock-in allele that lacked the C-terminal 31 amino acids and was very

similar to the mutations found in both individuals.[22] Mice homozygous for the mutant allele showed bone-marrow aplasia, short telomere lengths, abbreviated life expectancy, microcephaly, a small body size, and pulmonary fibrosis, a collection of characteristics that are essentially a phenocopy of DC. Hamard et al. reported that another mouse line expressing a truncated p53 lacking the C-terminal 24 amino acids presented similar phenotypes.[23] Both affected individuals described here shared several phenotypes, including bone marrow failure, microcephaly, and severe growth retardation (Table 1), with these mutant mice. However, there exist some differences between our cases and the mouse models. For example, telomere shortening was not prominent in either individual compared to typical DC-affected individuals with mutated *TERT*-related genes (Figure 1D).[11] Notably, although the heterozygous mice appeared to show minimal phenotypes, both individuals developed severe phenotypes even with a heterozygous *TP53* mutation. An hiPSC line carrying a heterozygous *TP53* mutation also showed impairment of erythrocyte production. It is unclear how these truncations (and augmented p53 functions) lead to the observed phenotype and exactly which of many p53 functions are affected by these mutations. Further studies are warranted to clarify these issues.

In conclusion, we identified germline *TP53* mutations in two cases of IBMFS. These mutations have not been previously described in humans. The p53 varaint was shown to have augmented p53 functions, rather than loss of function. The close similarities of genotypes and phenotypes among the individuals and the zebrafish, hiPSC and mouse models strongly suggest that the clinical phenotypes in our individuals could be explained by activated p53 functions caused by truncation of the C terminus. These findings will provide important insights into the previously postulated connection between p53 and IBMFSs.

Accession Numbers

The accession numbers for the sequences reported in this paper are ClinVar: SUB4310928, SUB4307372, SCV000786665.

Supplemental Data

Supplemental Data include a Supplemental Case Report, Supplemental Material and Methods, one figure, and three tables and can be found with this article online at https://doi.org/10.1016/j.ajhg.2018.07.020.

Acknowledgments

We would like to thank individuals 1 and 2 and their family members for making this work possible. This research used computational resources of the K computer provided by the RIKEN Advanced Institute for Computational Science through the HPCI System Research project (S.O.; hp150232). This work was supported by Practical Research Project for Rare/Intractable Diseases (JP17ek0109133), grants-in-aid (JP17ek0109099, JP16ck0106073, and JP17ek0109286s0101) from the Japan Agency for Medical Research and Development (AMED), and a research grant from the Ministry of Health, Labour, and Welfare of Japan (Research on Measures for Intractable Diseases) (201711031A) and Japan Society for the Promotion of Science KAKENHI grant number JP17K10093. S.O. was supported by the JSPS Core-to-Core Program, A. Advanced Research Networks.

Declaration of Interests

The authors declare no competing interests.

Received: May 16, 2018
Accepted: July 24, 2018
Published: August 23, 2018

Web Resources

European Genome-Phenome Archive, https://www.ebi.ac.uk/ega/home
Human Genetic Variation Browser, http://www.genome.med.kyoto-u.ac.jp/SnpDB/
NHLBI Exome Sequencing Project, http://evs.gs.washington.edu/EVS/
OMIM, http://www.omim.org/
ClinVar, https://www.ncbi.nlm.nih.gov/clinvar/
UCSC Genome Browser, https://genome.ucsc.edu/
PolyPhen-2, http://genetics.bwh.harvard.edu/pph2/
SIFT, http://sift.jcvi.org/

References

1. Bessler, M., Masson, P.J., Link, D.C., and Wilson, D.B. Inherited bone marrow failure syndrome. In Nathan and Oski's Hematology of Infancy and Childhood, 7th edition. S.H. Orkin, D.G. Nathan, D. Ginsburg, A.T. Look, D.E. Fisher, and S.E. Lux, eds. (W.B. Saunders), pp. 307–395.
2. Dutt, S., Narla, A., Lin, K., Mullally, A., Abayasekara, N., Megerdichian, C., Wilson, F.H., Currie, T., Khanna-Gupta, A., Berliner, N., et al. (2011). Haploinsufficiency for ribosomal protein genes causes selective activation of p53 in human erythroid progenitor cells. Blood *117*, 2567–2576.
3. Townsley, D.M., Dumitriu, B., and Young, N.S. (2014). Bone marrow failure and the telomeropathies. Blood *124*, 2775–2783.
4. Vlachos, A., Ball, S., Dahl, N., Alter, B.P., Sheth, S., Ramenghi, U., Meerpohl, J., Karlsson, S., Liu, J.M., Leblanc, T., et al.; Participants of Sixth Annual Daniella Maria Arturi International Consensus Conference (2008). Diagnosing and treating Diamond Blackfan anaemia: Results of an international clinical consensus conference. Br. J. Haematol. *142*, 859–876.
5. Sankaran, V.G., Ghazvinian, R., Do, R., Thiru, P., Vergilio, J.A., Beggs, A.H., Sieff, C.A., Orkin, S.H., Nathan, D.G., Lander, E.S., and Gazda, H.T. (2012). Exome sequencing identifies *GATA1* mutations resulting in Diamond-Blackfan anemia. J. Clin. Invest. *122*, 2439–2443.
6. Narla, A., and Ebert, B.L. (2010). Ribosomopathies: Human disorders of ribosome dysfunction. Blood *115*, 3196–3205.
7. Calado, R.T., and Young, N.S. (2009). Telomere diseases. N. Engl. J. Med. *361*, 2353–2365.

8. Jyonouchi, S., Forbes, L., Ruchelli, E., and Sullivan, K.E. (2011). Dyskeratosis congenita: A combined immunodeficiency with broad clinical spectrum–a single-center pediatric experience. Pediatr. Allergy Immunol. *22*, 313–319.
9. Vulliamy, T.J., Marrone, A., Knight, S.W., Walne, A., Mason, P.J., and Dokal, I. (2006). Mutations in dyskeratosis congenita: their impact on telomere length and the diversity of clinical presentation. Blood *107*, 2680–2685.
10. Khan, S., Pereira, J., Darbyshire, P.J., Holding, S., Doré, P.C., Sewell, W.A., and Huissoon, A. (2011). Do ribosomopathies explain some cases of common variable immunodeficiency? Clin. Exp. Immunol. *163*, 96–103.
11. Alter, B.P., Baerlocher, G.M., Savage, S.A., Chanock, S.J., Weksler, B.B., Willner, J.P., Peters, J.A., Giri, N., and Lansdorp, P.M. (2007). Very short telomere length by flow fluorescence in situ hybridization identifies patients with dyskeratosis congenita. Blood *110*, 1439–1447.
12. Kunishima, S., Okuno, Y., Yoshida, K., Shiraishi, Y., Sanada, M., Muramatsu, H., Chiba, K., Tanaka, H., Miyazaki, K., Sakai, M., et al. (2013). *ACTN1* mutations cause congenital macrothrombocytopenia. Am. J. Hum. Genet. *92*, 431–438.
13. Hug, N., Longman, D., and Cáceres, J.F. (2016). Mechanism and regulation of the nonsense-mediated decay pathway. Nucleic Acids Res. *44*, 1483–1495.
14. Kandoth, C., McLellan, M.D., Vandin, F., Ye, K., Niu, B., Lu, C., Xie, M., Zhang, Q., McMichael, J.F., Wyczalkowski, M.A., et al. (2013). Mutational landscape and significance across 12 major cancer types. Nature *502*, 333–339.
15. Malkin, D., Garber, J.E., Strong, L.C., and Friend, S.H. (2016). CANCER. The cancer predisposition revolution. Science *352*, 1052–1053.
16. Bouaoun, L., Sonkin, D., Ardin, M., Hollstein, M., Byrnes, G., Zavadil, J., and Olivier, M. (2016). TP53 variations in human cancers: New lessons from the IARC TP53 database and genomics data. Hum. Mutat. *37*, 865–876.
17. Ochi, K., Takayama, N., Hirose, S., Nakahata, T., Nakauchi, H., and Eto, K. (2014). Multicolor staining of globin subtypes reveals impaired globin switching during erythropoiesis in human pluripotent stem cells. Stem Cells Transl. Med. *3*, 792–800.
18. Feng, L., Lin, T., Uranishi, H., Gu, W., and Xu, Y. (2005). Functional analysis of the roles of posttranslational modifications at the p53 C terminus in regulating p53 stability and activity. Mol. Cell. Biol. *25*, 5389–5395.
19. Laptenko, O., Tong, D.R., Manfredi, J., and Prives, C. (2016). The tail that wags the dog: How the disordered C-terminal domain controls the transcriptional activities of the p53 tumor-suppressor protein. Trends Biochem. Sci. *41*, 1022–1034.
20. Huang, J., Perez-Burgos, L., Placek, B.J., Sengupta, R., Richter, M., Dorsey, J.A., Kubicek, S., Opravil, S., Jenuwein, T., and Berger, S.L. (2006). Repression of p53 activity by Smyd2-mediated methylation. Nature *444*, 629–632.
21. Wang, D., Kon, N., Lasso, G., Jiang, L., Leng, W., Zhu, W.G., Qin, J., Honig, B., and Gu, W. (2016). Acetylation-regulated interaction between p53 and SET reveals a widespread regulatory mode. Nature *538*, 118–122.
22. Simeonova, I., Jaber, S., Draskovic, I., Bardot, B., Fang, M., Bouarich-Bourimi, R., Lejour, V., Charbonnier, L., Soudais, C., Bourdon, J.C., et al. (2013). Mutant mice lacking the p53 C-terminal domain model telomere syndromes. Cell Rep. *3*, 2046–2058.
23. Hamard, P.J., Barthelery, N., Hogstad, B., Mungamuri, S.K., Tonnessen, C.A., Carvajal, L.A., Senturk, E., Gillespie, V., Aaronson, S.A., Merad, M., and Manfredi, J.J. (2013). The C terminus of p53 regulates gene expression by multiple mechanisms in a target- and tissue-specific manner in vivo. Genes Dev. *27*, 1868–1885.

The American Journal of Human Genetics, Volume *103*

Supplemental Data

De Novo Mutations Activating Germline *TP53* in an Inherited Bone-Marrow-Failure Syndrome

Tsutomu Toki, Kenichi Yoshida, RuNan Wang, Sou Nakamura, Takanobu Maekawa, Kumiko Goi, Megumi C. Katoh, Seiya Mizuno, Fumihiro Sugiyama, Rika Kanezaki, Tamayo Uechi, Yukari Nakajima, Yusuke Sato, Yusuke Okuno, Aiko Sato-Otsubo, Yusuke Shiozawa, Keisuke Kataoka, Yuichi Shiraishi, Masashi Sanada, Kenichi Chiba, Hiroko Tanaka, Kiminori Terui, Tomohiko Sato, Takuya Kamio, Hirotoshi Sakaguchi, Shouichi Ohga, Madoka Kuramitsu, Isao Hamaguchi, Akira Ohara, Hitoshi Kanno, Satoru Miyano, Seiji Kojima, Akira Ishiguro, Kanji Sugita, Naoya Kenmochi, Satoru Takahashi, Koji Eto, Seishi Ogawa, and Etsuro Ito

Supplemental Note: Case Reports

Individual 1 was a male born at term after an uncomplicated pregnancy to healthy, unrelated parents. Birth weight was 2,972g (−0.7 SD), height 48.2 cm (−0.8 SD), and head circumference 31.7 cm (−1.3 SD). There was no family history of mental or hematological disorders. At 1 month of age, he visited a hospital because of intractable diarrhea, at which point hypogammaglobulinemia (IgG 1.53 g/L) was recognized. Anemia was noted at 2 months of age, when complete blood counts (CBC) showed hemoglobin 59 g/L, mean corpuscular volume (MCV) 103.5 fL, a white blood cell (WBC) count of 11.1 × 10^9/L with normal differential counts, platelet count 583 × 10^9/L, and 0.1% reticulocytes. Laboratory tests confirmed hypogammaglobulinemia, IgG 0.2 g/L, IgA 0.05 g/L and IgM 0.09 g/L. Bone marrow aspiration showed severe selective erythroid hypoplasia with otherwise normal cellularity. Chromosomal analysis showed normal karyotype (46XY, 9gh+). At 3 months of age, he had an episode of tonic-clonic seizure. He was diagnosed as having epilepsy and anticonvulsants were initiated with limited efficacy. At 5 months of age, regular IgG replacement and red blood cell transfusions were initiated. At one year of age, DBA was considered the probable diagnosis, and he was treated with methylprednisolone pulse therapy without improvement. At 6 years of age CD19+ B cells and CD3+ T cells were 2% and 97%, respectively. $CD19^+$ B cells were progressively decreased to 0.3% at 12 years of age, whereas CD3+ T cells remain unchanged (98%). He received chronic transfusion therapy to maintain a hemoglobin level above 60 g/L. He developed secondary hemochromatosis due to transfusional iron overload and chelation therapy was initiated from 8 years of age. He had hypothyroidism due to hemochromatosis and thyroid hormone replacement therapy was initiated. At 13 years of age, his anemia showed a spontaneous remission and he became transfusion-independent, although the platelet counts gradually decreased from 12 years of age (51 x 10^9/L). He was suspected of having DBA. However, no mutations were detected in the known DBA genes.[1,2] The activity of erythrocyte adenosine deaminase was normal (1.24 IU/gHb) and the erythrocyte reduced glutathione concentration was not elevated (81.4 mg/dLRBC).[3] Bone marrow analysis revealed hypocellurarity and mild tri-lineage dysplasia, which was consistent with refractory cytopenia of childhood.[4] The growth chart showed severe retardation. He had reticular skin pigmentation, tooth anomalies and hypogonadism with atrophy of the testis. He had severe microcephaly and general psychomotor

retardation: his head circumference as of 16 years of age was 42.0 cm (< −6.0 SD). Although he shared some features of DC, telomeres were not significantly shortened compared to typical DC cases with mutant *TERT*-related genes. He is now 20 years old. However, his bone age is that of a 12–year-old due to hypogonadism and he continues growing slowly. Although he remains transfusion-independent, he needs regular IgG replacement therapy for persistent hypogammaglobulinemia. No cancers were identified in this individual.

Individual 2 was a male born to healthy, unrelated parents. Pregnancy had been full-term and uncomplicated. Birth weight was 2,412 g (−1.4 SD), height 50 cm (+0.5 SD), and head circumference 31 cm (−1.6 SD). Anemia was first noticed at 5 days of age. There was no family history of mental or hematological disorders. He was referred to our hospital at 15 days of age. CBC showed the following: hemoglobin, 51 g/L; MCV, 99.4 fL; WBC, 6.84 × 10^9/L with normal differential counts; platelets, 357 × 10^9/L; and 0.6% reticulocytes. Bone marrow examination showed selective erythroid hypoplasia (5%). Chromosome analysis revealed a normal 46,XY karyotype and chromosome fragility test with mitomycin C was normal. Telomere shortening was not remarkable. From 1 month of age, he became transfusion-dependent and required a regular red cell transfusion every 4 to 5 weeks. At 9 months of age he had an afebrile convulsion, for which an anticonvulsant was initiated. At that time he was found to have hypogammaglobulinemia (IgG 2.92 g/L, IgA 0.01 g/L and IgM 0.05 g/L), for which regular IgG replacement was initiated. CD19+ B cells and CD3+ T cells were 19.2% and 72.7%, respectively. DBA was considered as a probable diagnosis for the cause of pure red cell anemia, and steroid therapy was initiated. However, his anemia did not respond to prednisolone (2 mg/kg/day). No mutations were detected in the known DBA genes.[1,2] Growth was severely retarded. He had severe microcephaly and general psychomotor retardation: as of 5 years of age, his head circumference was 42.7 cm (−4.9 SD). Because of a persistent Norovirus infection with a duration of 2 years, he underwent bone marrow transplantation from an HLA-matched unrelated donor at 7 years of age. However, he died of interstitial pneumonia with chronic graft-versus-host disease 250 days after transplantation. No cancers were identified in this individual.

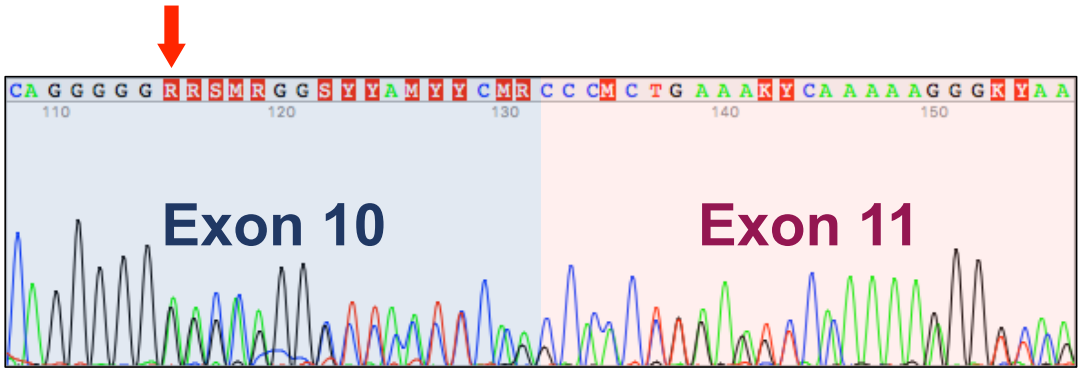

Figure S1. Sanger sequencing detected the mutant transcripts at a comparable level to normal transcripts in peripheral blood mononuclear cells from Individual 1. Arrowhead indicates the position of single nucleotide deletion at c.1083G.

Supplementary Table 3. Erythroid differentiation of human iPS cells carrying a heterozygous *TP53* mutant allele that lacked the C-terminal 32 amino acid.

Experiment 1

Day		Totall cell number (A)	Glycophorin A-positive cells (B)	Red cells (A*B)
0	WT	2.00E+04		2.00E+04
	hetero	2.00E+04		2.00E+04
6	WT	4.56E+05	0.7352	3.35E+05
	hetero	5.28E+05	0.871	4.60E+05
12	WT	3.93E+06	0.9688	3.80E+06
	hetero	2.00E+06	0.9367	1.87E+06
18	WT	2.25E+06	0.924	2.08E+06
	hetero	9.38E+05	0.785	7.36E+05

Experiment 2

Day		Totall cell number (A)	Glycophorin A-positive cells (B)	Red cells (A*B)
0	WT	2.00E+04		2.00E+04
	hetero	2.00E+04		2.00E+04
6	WT	4.64E+05	0.932158	4.33E+05
	hetero	2.50E+05	0.780205	1.95E+05
12	WT	4.55E+06	0.9585	4.36E+06
	hetero	2.30E+06	0.9471	2.18E+06
18	WT	2.00E+06	0.9691	1.94E+06
	hetero	5.00E+05	0.9643	4.82E+05

Experiment 3

Day		Totall cell number (A)	Glycophorin A-positive cells (B)	Red cells (A*B)
0	WT	2.00E+04		2.00E+04
	hetero	2.00E+04		2.00E+04
6	WT	7.10E+05	0.92837	6.59E+05
	hetero	5.00E+05	0.80994	4.05E+05
12	WT	4.90E+06	0.99314	4.87E+06
	hetero	2.37E+06	0.99034	2.35E+06
18	WT	2.87E+06	0.9846	2.83E+06
	hetero	1.00E+06	0.9783	9.78E+05

Supplemental Materials and Methods

Sample preparation

Genomic DNA was extracted from peripheral blood (PB) using a QIAamp DNA Blood Mini kit (QIAGEN, Hilden, Germany), according to the manufacturer's instructions.

Whole exome-sequencing and detection of germline mutations

For exome sequencing, genomic DNA from each member of the two pedigrees was enriched for protein-coding sequences with a SureSelect Human All Exon V3, V4 or V5 kit (Agilent Technologies, Santa Clara, CA, USA). This isolation was followed by massively parallel sequencing with the HiSeq 2000 platform with 100 bp paired-end reads (Illumina, San Diego, CA, USA). Candidate germline variants were detected through our in-house pipeline for exome-sequencing analysis with minor modifications for the detection of germline variants.[5] The resultant sequences were aligned to hg19 using the Burrows-Wheeler Aligner.[6] After removal of duplicate artifacts caused by PCR, the single nucleotide variants with allele frequencies > 0.25 and insertion-deletions with allele frequencies > 0.2 were called. With a mean coverage of 98.5× (79×–125×), > 92% of the 50 Mb target sequences were analyzed by > 10 independent reads.

Measurements of telomere length

The average relative telomere length (RTL) of peripheral lymphocytes was measured by flow-fluorescence *in situ* hybridization (flow-FISH), using a Telomere PNA kit (Dako Cytomation, Glostrup, Denmark). Details of the technical methods can be found in Baerlocher et al.[7] Briefly, peripheral blood lymphocytes were isolated by Ficoll separation and denatured in formamide at 82°C, hybridized with a fluorescein-conjugated $(CCCTAA)_3$ peptide nucleic acid probe and counterstained with LDS751 DNA dye. The analysis of fluorescence was performed using a FACSCalibur flow cytometer (Becton Dickinson Biosciences, San Jose, CA). After gating on diploid cells based on staining with propidium iodine, lymphocytes were isolated on the basis of size and granularity. Relative telomere length (RTL) was calculated as the ratio between the telomere signal of each sample and that of the control (cell line 1301) using the following formula: (mean FL1 of sample cells with probe – mean FL1 of sample cells without probe) × DNA index of control cells / (mean FL1 of control cells with probe – mean FL1 control cells without probe) × DNA index of sample cells.

Construction of plasmids

To introduce the *TP53* mutations derived from Individuals 1 (c.1077delA) and 2 (c.1083delG) into the p53 pcDNA3.1 vector,[8] we performed inverse PCR (Primer STAR: Takara Bio) with the primer pair 45A-F (5' – GAGCCGGGGGGAGCAGGGCTCACTCCAGCCACCTGAAG- 3') and 45R (5' – CCTTCCCAGCCTGGGCATCCTTGAGTTCCAAGGCCTCA- 3') or 124G-F (5' – GAGCCGGGGGAGCAGGGCTCACTCCAGCCACCTGAAG-3') and 45R. PCR products were self-ligated and cloned to TP53 c.1077 pcDNA3.1 or TP53 c.1083 pcDNA3.1 expression vector.

For promoter assays, the luciferase reporter plasmid PICA p21–2.3k was constructed as follows.[8] A fragment containing 2.3 kb of the *CDKN1A* promoter region was amplified from CMK11-5 genomic DNA by PCR using the primers 5'-AGGGTACCAGGAACATGCTTGGGCAGC-3' and 5'-TGAAGCTTCCGGCTCCACAAGGAACTGA-3'. The PCR products were digested with *Kpn*I and *Hind*III, then subcloned into the PICA gene basic vector (Toyo Ink, Tokyo, Japan).

Reporter assay

The human osteosarcoma cell line MG-63 and quail fibroblast cell line QT6 were maintained in Eagle's minimal essential medium (MEM) with non-essential amino acids and 10% fetal bovine serum (FBS) at 37℃ in 5% CO_2. Cells were seeded at a density of 2 x 10^4 cells/well (24 well plate). Following overnight culture, MG63 cells were transfected with 3 μL FuGENE HD transfection reagent (Promega, Fitchburg, WI) whereas QT6 cells received 1.5 μL of reagent according to the manufacturer's protocol. The transfection mixtures contained 400 ng (for MG-63) or 200 ng (for QT6) of firefly luciferase reporter plasmid, 600 ng (for MG-63) or 300 ng (for QT6) of plasmids expressing wild-type or mutant p53. *Renilla* luciferase expressing vector, pEF-Seapansy, was also transfected as a normalization control. Cells were collected 24 h after the transfection, and luciferase activity was measured using the Dual-Luciferase Reporter Assay System (Promega).

Functional analysis using zebrafish

A Morpholino antisense oligo (MO) targeting the intron 10/exon 11 boundary of zebrafish *tp53* was obtained from Gene Tools, LLC (Philomath, OR, USA). The sequence was TGTCATGCTGAAAGAAAAAGAATGA. The MO was injected at a concentration of 1.0, 2.5 or 5.0 μg/μL into single-cell stage embryos. The MO-injected embryos were grown at 28.5°C. Hemoglobin staining was performed at 48 h post-fertilization (hpf) using *o*-dianisidine.[9]

Total RNA was isolated from wild-type and the MO-injected embryos at 8 hpf. Reverse transcription (RT)-PCR was used to distinguish normal and intron-containing sizes of the *tp53* transcripts. This was performed by using a primer pair designed at exons 8 and 11. The primer sequences were 5'- ACCACTGGGACCAAACGTAG -3' (exon8) and 5'- AAATGACCCCTGTGACAAGC -3' (exon11).

Gene targeting of human iPSCs

The plasmids expressing CRISPR guide RNA and Cas9 were prepared by ligating oligos into the BbsI site of pX330 (Addgene no. 42230). CRISPR guide sequences were designed using web resources to introduce frame-shift mutations in the C-terminal domain (CTD) of *TP53*. The targeting constructs for genome editing and neomycin resistance gene expression plasmids were transfected into human induced pluripotent stem cells #8 (hiPSCs #8)[10] using FuGENE HD transfection reagent (Promega, Fitchburg, WI) and selected with neomycin (G418). Drug-resistant clones were manually transferred into 96-well plates and expanded for genomic DNA extraction and continued culture. Targeted clones were identified by PCR.

Real-time-quantitative reverse transcription PCR

For analysis of gene expression, the iScript System (Bio-Rad, Hercules, CA, USA) was used to synthesize single strand cDNA from 100 ng of total RNA isolated from hiPSC lines using an RNeasy Mini kit (Qiagen, Hilden, Germany) according to the manufacturer's instructions. Each cDNA was used for real-time quantitative PCR. Reactions were performed using iQ SYBR Green Supermix (Bio-Rad) on a CFX system (Bio-Rad). Gene-specific primers for *GAPDH*, *CDKN1A*, *MDM2*, *PMAIP1* and *TIGAR* were selected from the Perfect Real Time Support System (TAKARA Bio, Kusatsu, Japan). The amplification program consisted of 1 cycle of 95°C for 3 min and then 40

cycles of 95°C for 5 s, 60°C for 20 s. Gene expression levels were normalized against the level of the *GAPDH* gene.

Erythroid differentiation via sac-formation from human iPSCs

To differentiate hiPSCs into erythroid cells, we used our previously established protocol.[10] In brief, basic differentiation medium contained IMDM (Sigma-Aldrich, MO, USA) supplemented with 15% FBS, L-glutamine (Thermo, MD, USA), insulin-transferrin-selenium (Thermo), 50 μg/mL ascorbic acid (Sigma-Aldrich), and 450 μM 1-thioglycerol (Sigma-Aldrich). Small clumps of hiPSCs (< 200 cells) were cultivated on C3H10T1/2 stromal cells in basic differentiation medium supplemented with 20 ng/mL human VEGF (R&D) to obtain CD34+ cells at day 14. To further induce erythroid lineage cells, $CD34^+$ cells at day 14 were purified by flow cytometry (FACS Aria II, BD Bioscience, CA). Aliquots of the $CD34^+$ cells (2×10^4) were then transferred onto fresh C3H10T1/2 stromal cells and maintained in basic differentiation medium with 50 ng/mL SCF (R&D), 50 ng/mL TPO (R&D), and 5 U/mL EPO (KYOWA KIRIN, Tokyo, Japan), until Ery phase Day 6 (total of 20 days from the hiPSC stage). From Ery Day 6 to Day 12 (total of 26 days) or Day 18 (32 days), the cells were cultured in the presence of 5 U/mL EPO alone. Non-adherent cells were collected and analyzed at Ery Days 6, 12, and 18. Cell growth was analyzed by flow cytometry (FACS Aria II, BD Bioscience, San Diego, CA).

Supplemental References

1. Konno, Y., Toki, T., Tandai, S., Xu, G., Wang, R., Terui, K., Ohga, S., Hara, T., Hama, A., Kojima, S., et al. (2010). Mutations in the ribosomal protein genes in Japanese patients with Diamond-Blackfan anemia. Haematologica *95*,1293-1299.
2. Kuramitsu, M., Sato-Otsubo, A., Morio, T., Takagi, M., Toki, T., Terui, K., Wang, R., Kanno, H., Ohga, S., Ohara, A., et al. (2012). Extensive gene deletions in Japanese patients with Diamond-Blackfan anemia. Blood *119*, 2376-2384.
3. Utsugisawa, T., Uchiyama, T., Toki, T., Ogura, H., Aoki, T., Hamaguchi, I., Ishiguro, A., Ohara, A., Kojima, S., Ohga, S., Ito, E., and Kanno H. (2016). Erythrocyte glutathione is a novel biomarker of Diamond-Blackfan anemia. Blood Cells Mol Dis *59*, 31-36.
4. Arber, D.A., Orazi, A., Hasserjian, R., Thiele, J., Borowitz, M.J., Le Beau, M.M., Bloomfield, C.D., Cazzola, M., and Vardiman, J.W. (2016). The 2016 revision to the World Health Organization classification of myeloid neoplasms and acute leukemia. Blood *127*, 2391-2405.
5. Kunishima, S., Okuno, Y., Yoshida, K., Shiraishi, Y., Sanada, M., Muramatsu, H., Chiba, K., Tanaka, H., Miyazaki, K., Sakai, M., et al. (2013). *ACTN1* mutations cause congenital macrothrombocytopenia. Am J Hum Genet *92*, 431-438.
6. Li, H., and Durbin, R. (2009). Fast and accurate long-read alignment with Burrows-Wheeler transform. Bioinformatics *25*,1754–1760.
7. Baerlocher, G.M., Vulto, I., de Jong, G., and Lansdorp, P.M. (2006). Flow cytometry and FISH to measure the average length of telomeres (flow FISH). Nature Protoc. *1*,2365-2376.
8. Kanezaki, R., Toki, T., Xu, G., Narayanan, R., ad Ito, E. (2006). Cloning and characterization of the novel chimeric gene p53/FXR2 in the acute megakaryoblastic leukemia cell line CMK11-5. Tohoku J Exp Med *209*,169-180.
9. Uechi, T., Nakajima, Y., Nakao, A., Torihara, H., Chakraborty, A., Inoue, K., and Kenmochi, N. (2006). Ribosomal protein gene knockdown causes developmental defects in zebrafish. PLoS One *1*,e37.
10. Ochi, K., Takayama, N., Hirose, S., Nakahata, T., Nakauchi, H., and Eto, K. (2014). Multicolor staining of globin subtypes reveals impaired globin switching during erythropoiesis in human pluripotent stem cells. Stem Cells Transl Med. *3*,792-800.